NASA Technical Memorandum 4262

Corrections to the Participant-Spectator Model of High-Energy Alpha-Particle Fragmentation

Francis A. Cucinotta, Lawrence W. Townsend,
John W. Wilson, and John W. Norbury

MAY 1991

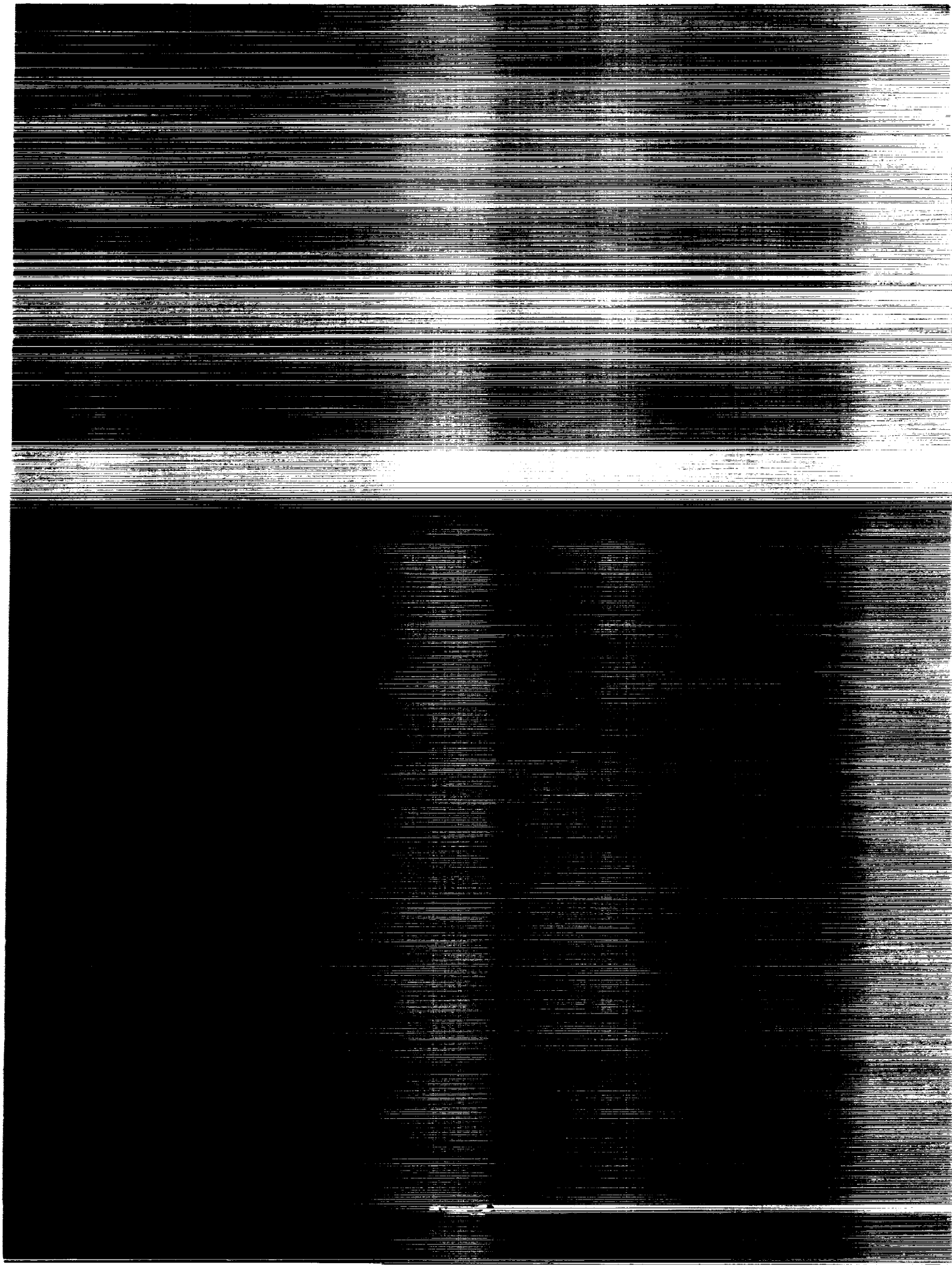

NASA Technical Memorandum 4262

Corrections to the Participant-Spectator Model of High-Energy Alpha-Particle Fragmentation

Francis A. Cucinotta, Lawrence W. Townsend,
and John W. Wilson
Langley Research Center
Hampton, Virginia

John W. Norbury
Rider College
Lawrenceville, New Jersey

National Aeronautics and
Space Administration
Office of Management
Scientific and Technical
Information Division

1991

Symbols and Notation

Particles and fragments:

a, b	projectile fragments
N	nucleon
n	neutron
P	projectile
p	proton
T	target
v	virtual particle
X	final target state
α	alpha particle

Symbols:

A_i	mass number of particle i
B	slope parameter
D_i	energy of particle i in center-of-mass frame
$D(p,q)$	dispersion integral (eq. (20))
E_i	energy of particle i
FSI	final-state interactions
f_{iT}	scattering amplitude of fragment i
i	imaginary number
K	phase space factor
K_i	4-momentum of virtual particle i
K_s, K_p	defined in equations (9) and (12)
$\mathbf{k}_i$	momentum of virtual particle i
$\mathbf{k}_{ij}$	relative momentum of virtual particles i and j
$\mathbf{k}$, $\mathbf{k}'$	intermediate-state relative momenta (eqs. (17) and (18))
m_i	mass of particle i
P_i	4-momentum of particle i
$\mathbf{p}_i$	momentum of particle i
$\mathbf{p}_{ij}$	relative momentum of particles i and j
p_{lab}	laboratory momentum, MeV
$\mathbf{Q}$	total momentum transfer
$\mathbf{R}_i$	momentum of particle i in center-of-mass frame
T_D^1, T_D^2	double-scattering contribution to transition matrix
T_s, T_p	contributions to transition matrix from spectator and participant terms
$\widetilde{T}_s, \widetilde{T}_p$	distorted transition matrix contributions
t_{ij}	full transition amplitudes for interaction between particles i and j
V	normalization volume
Y_s, Y_p	defined in equations (10) and (13)
α	$= -2\mu_{ab}\epsilon_s$
β_{ij}	relative velocity between particles i and j
ϵ	infinitesimal energy
ϵ_s	separation energy
θ_i	emission angle of particle i
θ_{lab}	laboratory emission angle, deg
μ_{ij}	reduced mass of particles i and j
ρ	ratio of the real to imaginary parts of the forward scattering amplitudes
σ	cross section, mb
Φ	relative cluster momentum distribution
$\tilde{\Phi}$	distorted relative cluster momentum distribution
ϕ	overlap function
Ω_i	solid angle of emission of particle i

Abstract

The participant-spectator model of nuclear fragmentation is described in terms of pole graphs from direct reaction theory. Corrections to the model for more than one projectile fragment scattering on the target are considered using a triangle graph model. Results for alpha-particle fragmentation at 1 GeV/A indicate that corrections to the participant-spectator model are significant, as indicated by the large interference effects found between the pole and triangle graph terms in the double- and single-differential cross sections.

Introduction

The description of biological damage from galactic cosmic rays (GCR) ultimately depends on the track structure of energetic ions in tissue (refs. 1 and 2). Risk assessment for deep space missions requires accurate transport codes for determining the differential flux of ions behind natural and protective radiation shielding. Previous studies (refs. 3 and 4) have indicated the importance of the nuclear fragmentation data base in developing such transport codes. Nuclear fragmentation drastically alters the composition of ion fields, and its proper description is essential for track structure models or any fluence-based risk system.

For high-energy reactions, the participant-spectator model (ref. 5) describes the dominant peripheral channels where only a small number of projectile fragments are produced. These move in the forward direction with velocities near that of the projectile. The nuclear abrasion process occurs for large impact parameters when the overlapping volumes of the projectile and target nuclei, called participants, are sheared off in the collision. The remaining portion of the projectile, the spectator, is assumed to receive only a small momentum transfer in the collision. The spectator fragment may be in an intermediate excited state (prefragment stage), decaying to the final fragment through particle evaporation in the ablation step of the reaction. In contrast to the peripheral breakup channels, there are central collisions when almost complete overlap of projectile and target volumes leads to a multiplicity of fragments in a wide cone of emission angles.

In previous work (refs. 6 and 7), we have considered the diagram approach to direct reaction theory (ref. 8) for describing the abrasion step in terms of dispersion pole diagrams. In this work, we consider corrections to the pole diagrams for two-body dissociation in order to estimate contributions when more than one projectile fragment interact strongly (participate) in the reaction. The direct reaction graphs with singularities closest to the physical values of the fragment variables give the dominant contributions to the cross sections. For the direct reaction approach to be useful, only a few dispersion graphs should contribute over the kinematical region of interest. In references 6 and 7, we showed that the single-pole diagram corresponding to the participant-spectator assumption saturates the production cross section only if the mass of the fragment of interest is much larger than that of the participant fragments. For the lightest nuclei, and for some dissociation channels for heavier projectiles, fragments with comparable mass are produced in a single channel. Rescattering corrections may then become important and are investigated herein for ^{4}He projectiles (alpha particles) fragmenting on ^{1}H targets. For heavier systems, the multiple scattering approach considered here is expected to be modified by using the high-energy optical model (refs. 9 and 10) to properly account for distortion and cascade effects and by treating the ablation step according to the methods in reference 11.

Pole Diagrams

Consider the two-body dissociation of a projectile P fragmenting on a target T:

$$P + T \rightarrow a + b + X \tag{1}$$

where X is the final target state, and a and b are the projectile fragments. The transition matrix T_{fi} for this reaction is related to the momentum distribution for producing the fragment a by

$$\frac{d\sigma}{d\mathbf{p}_a} = \frac{V^3}{(2\pi)^5 \beta_{PT}} \int d\Omega_b \, K |T_{fi}|^2 \tag{2}$$

where β is the relative velocity in the initial state, K is the phase space factor, and V is the normalization volume; a summation over all final target states X is implied. In the overall center-of-mass frame (CM),

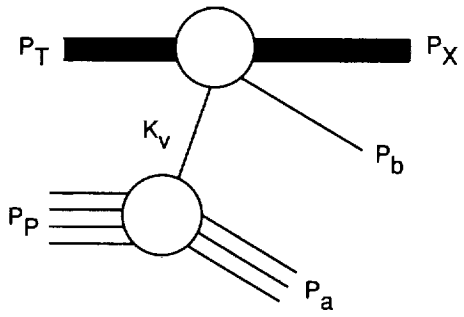

Figure 1. Spectator term for projectile fragmentation.

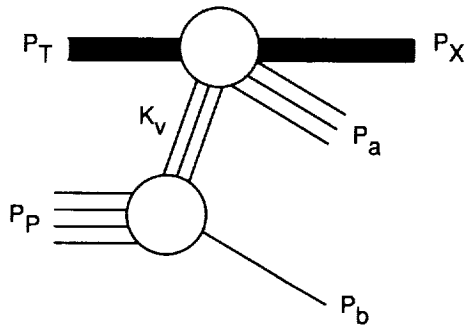

Figure 2. Participant term for projectile fragmentation.

assuming azimuthal symmetry about the beam direction, we have

$$K = \frac{p_b^2 E_b E_X}{p_b(E_b + E_X) + p_a E_b \cos(\theta_a + \theta_b)} \tag{3}$$

The pole diagram for the spectator contribution (Serber term), where the observed fragment is assumed to avoid interaction with the target, is shown in figure 1. A first correction to the spectator model is to reverse the roles of the participant and spectator, with the observed fragment interacting with the target as shown in figure 2. These terms have simple poles at the value of the interacting fragment's mass (ref. 8) and both contribute at small $\mathbf{p}_a$ if the masses, m_a and m_b, are comparable (refs. 6 and 7). Here the singularities of both graphs are relatively close to the physical region. Similar conclusions are expected if the Treiman-Yang criterion (ref. 12) is used to test the spectator pole term. The spectator contribution to the transition matrix is written

$$T_s = \phi\left(\mathbf{p}_a - \frac{A_a}{A_P}\mathbf{p}_P\right) t_{bT}(\mathbf{Q}) \tag{4}$$

and the participant contribution is written

$$T_p = \phi\left(-\mathbf{p}_b + \frac{A_b}{A_P}\mathbf{p}_P\right) t_{aT}(\mathbf{Q}) \tag{5}$$

where ϕ is the overlap function for the virtual dissociation of the projectile, $\mathbf{Q}$ is the total momentum transfer, and t_{iT} is the full transition amplitude for the fragment-target interaction. In equations (4) and (5), we are using the high-energy (on-shell) approximation, and all amplitudes are evaluated at the initial energy. Note that the total momentum transfer is

$$\mathbf{Q} = \mathbf{p}_T - \mathbf{p}_X = \mathbf{p}_a + \mathbf{p}_b - \mathbf{p}_P \tag{6}$$

and the relative momentum of the fragments is

$$\mathbf{p}_{ab} = \frac{1}{A_P}(A_b\mathbf{p}_a - A_a\mathbf{p}_b) \tag{7}$$

The amplitudes appearing in the pole diagrams are transformed to their proper CM frames using relativistic kinematics and the Moller invariants such that

$$T_s = \frac{-2\pi}{V}\sqrt{K_s}\sqrt{Y_s}\,\phi(\mathbf{R}_a)\, f_{bT}(\mathbf{R}_\mathbf{Q}) \tag{8}$$

where f is the scattering amplitude,

$$\sqrt{K_s} = \left[\frac{D_T D_b D_X (D_P - D_a)}{E_T E_b E_X (E_P - E_a)}\right]^{1/2}\left[\frac{\mathbf{R}_{bT}(D_b + D_X)}{\beta_{bT} D_b D_X}\right]^{1/2} \tag{9}$$

and

$$\sqrt{Y_s} = \left[\frac{m_P D_a (m_P - D_a)}{E_P E_a (E_P - E_a)}\right]^{1/2} \tag{10}$$

For the participant term, we have

$$T_p = \frac{-2\pi}{V}\sqrt{K_P}\sqrt{Y_P}\,\phi(-\mathbf{R}_b)\, f_{aT}(\mathbf{R}_\mathbf{Q}) \tag{11}$$

where

$$\sqrt{K_p} = \left[\frac{D_T D_a D_X (D_P - D_b)}{E_T E_a E_X (E_P - E_b)}\right]^{1/2}\left[\frac{\mathbf{R}_{aT}(D_a + D_X)}{\beta_{aT} D_a D_X}\right]^{1/2} \tag{12}$$

and

$$\sqrt{Y_p} = \left[\frac{m_P D_b (m_P - D_b)}{E_P E_b (E_P - E_b)}\right]^{1/2} \tag{13}$$

In equations (8) through (13), D and $\mathbf{R}$ denote energies and momenta in the proper CM frame, which may differ for each amplitude.

The contribution of the pole terms to the momentum distribution is now written

$$\frac{d\sigma}{d\mathbf{p}_a} = \frac{1}{\beta_{PT}}\int d\Omega_b\, K\Big|-\sqrt{K_s Y_s}\,\Phi(\mathbf{R}_a)\, f_{bT}(\mathbf{R}_\mathbf{Q}) - \sqrt{K_p Y_p}\,\Phi(-\mathbf{R}_b)\, f_{aT}(\mathbf{R}_\mathbf{Q})\Big|^2 \tag{14}$$

where we have defined the relative cluster momentum distribution

$$\Phi(\mathbf{R}) = \frac{\sqrt{V}}{(2\pi)^{3/2}}\phi(\mathbf{R}) \tag{15}$$

Final-State Interactions

The fragments a and b are expected to interact following their separation, and their relative momentum vector is expected to have a relatively small value. The diagrams for final-state interactions (FSI) between projectile fragments are shown in figures 3 and 4. Following references 13 to 15, we use a separable potential model that incorporates orthogonality between the bound and scattering states of the projectile fragments and that is appropriate for small $\mathbf{p}_{ab}$. Note that orthogonality is violated if an optical potential is employed, since the same potential is not employed to describe the bound and scattering states.

For figure 3, we write

$$T_s^{\mathrm{FSI}} = t_{bT}(\mathbf{Q})\frac{V}{(2\pi)^3}\int d\mathbf{k}'\frac{2\mu_{ab}\,\phi(\mathbf{k})\,t_{ab}(\mathbf{k},\mathbf{k}')}{\mathbf{p}_{ab}^2 - \mathbf{k}'^2 + i\epsilon} \tag{16}$$

where μ is reduced mass and we define the intermediate-state relative momenta

$$\mathbf{k} = \frac{1}{A_P}\left(A_b\mathbf{k}_a - A_a\mathbf{k}_v\right) \tag{17}$$

and

$$\mathbf{k}' = \frac{1}{A_P}\left(A_b\mathbf{k}_a - A_a\mathbf{k}_b\right) \tag{18}$$

Following references 13 to 15, we use the separable potential model for t_{ab} such that equation (16) is reduced to

$$T_s^{\mathrm{FSI}} = \frac{2\pi}{V}\sqrt{K_s}\sqrt{Y_s}\,\Phi(\mathbf{R}_{ab})\frac{D\left(\mathbf{R}_{ab}, 2\frac{A_a}{A_P}\mathbf{R}_{\mathbf{Q}}\right)}{D(\mathbf{R}_{ab},0)}f_{bT}(\mathbf{R}_{\mathbf{Q}}) \tag{19}$$

where the dispersion integral is defined in reference 14 as

$$D(p,q) = \int d\mathbf{k}\frac{\Phi(\mathbf{k}+\mathbf{q}/2)\left(\alpha^2+k^2\right)\Phi(\mathbf{k})}{p^2-k^2+i\epsilon} \tag{20}$$

and α is related to the a-b separation energy ϵ_s through $\alpha^2 = -2\mu_{ab}\epsilon_s$. The dispersion integral is evaluated in analytic form for typical phenomenological forms of the overlap functions.

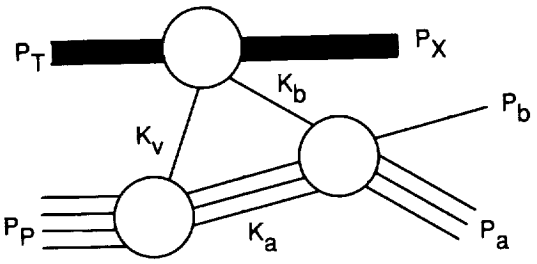

Figure 3. Spectator term with final-state interaction.

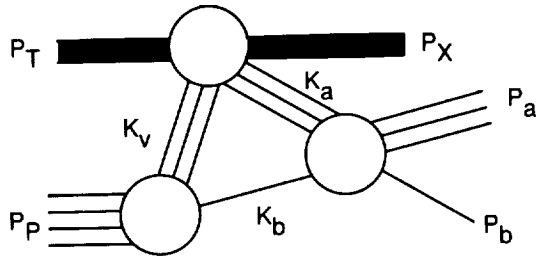

Figure 4. Participant term with final-state interaction.

We now define a distorted momentum distribution given by

$$\tilde{\Phi}(\mathbf{R}_a,\mathbf{R}_{ab}) = \Phi(\mathbf{R}_a) - \Phi(\mathbf{R}_{ab})\frac{D(\mathbf{R}_{ab}, 2\frac{A_a}{A_P}\mathbf{R}_{\mathbf{Q}})}{D(\mathbf{R}_{ab},0)} \tag{21}$$

and the distorted spectator term

$$\begin{aligned}\tilde{T}_s &= T_s + T_s^{\mathrm{FSI}} \\ &= \frac{-2\pi}{V}\sqrt{K_sY_s}\,\tilde{\Phi}(\mathbf{R}_a,\mathbf{R}_{ab})\,f_{bT}(\mathbf{Q})\end{aligned} \tag{22}$$

Similarly for the participant contribution

$$\begin{aligned}\tilde{T}_p &= T_p + T_p^{\mathrm{FSI}} \\ &= \frac{-2\pi}{V}\sqrt{K_pY_p}\,\tilde{\Phi}(\mathbf{R}_b,\mathbf{R}_{ab})\,f_{aT}(\mathbf{Q})\end{aligned} \tag{23}$$

Evaluation of these terms for model inputs is discussed subsequently. The pole model with FSI for the fragment momentum distribution is now written as in equation (14) with the distorted terms discussed above replacing the relative cluster momentum distributions.

Double-Scattering Corrections

The corrections to the pole diagrams for scattering by a second projectile fragment on the target are shown in figures 5 and 6. Figures 7 and 8 show further contributions from FSI between a and b. The contributions from the graphs in figures 7 and 8 are expected to be difficult to evaluate, since

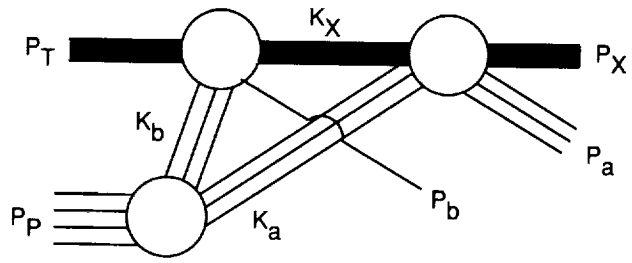

Figure 5. Rescattering correction for spectator term for projectile fragmentation.

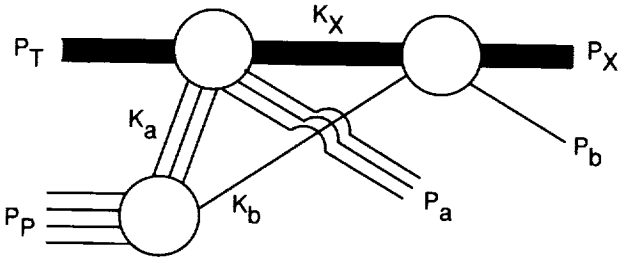

Figure 6. Rescattering correction for participant term for projectile fragmentation.

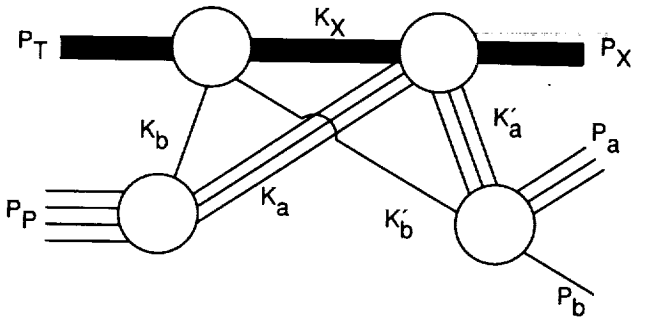

Figure 7. Rescattering correction for spectator term with final-state interaction.

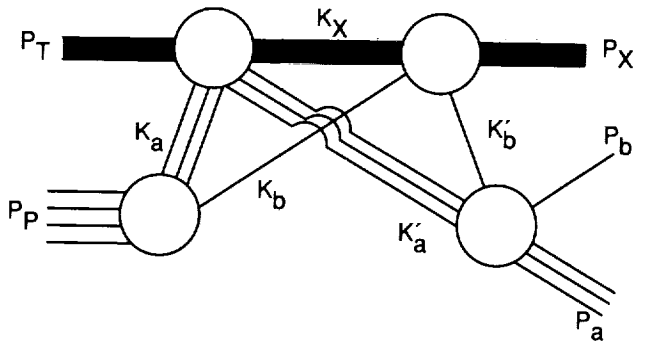

Figure 8. Rescattering correction for participant term with final-state interaction.

the complications of a three-body propagator cannot be avoided, even in the cluster model employed herein. The contributions from the double-scattering diagrams of figures 5 and 6 are estimated using the high-energy propagator derived in reference 9.

Define the relative momenta for figure 5 to be

$$\mathbf{p}_{aX} = \frac{1}{A_T + A_a}\left(A_a \mathbf{p}_X - A_T \mathbf{p}_a\right) \tag{24}$$

and

$$\mathbf{k}_{aX} = \frac{1}{A_T + A_a}\left(A_a \mathbf{k}_X - A_T \mathbf{k}_a\right) \tag{25}$$

and the momentum transfers to be

$$\mathbf{q}_1 = \mathbf{p}_T - \mathbf{k}_X \tag{26}$$

and

$$\mathbf{q}_2 = \mathbf{k}_X - \mathbf{p}_X \tag{27}$$

with

$$\mathbf{k}_{aX} = \mathbf{p}_{aX} + \mathbf{q}_2 \tag{28}$$

We write the double-scattering contribution to the transition matrix of figure 5 as

$$T_D^1 = \frac{V}{(2\pi)^3}\int d\mathbf{k}_{aX}\,\frac{2\mu_{aT}\, t_{bT}(\mathbf{q}_1)\,\phi(\mathbf{k}_{ab})\, t_{aT}(\mathbf{q}_2)}{\mathbf{p}_{aX}^2 - \mathbf{k}_{aX}^2 + i\epsilon} \tag{29}$$

Ignoring the noninvariance of the amplitudes on the right side of equation (29), we approximate this expression by

$$T_D^1 \approx \frac{1}{\pi V \mu_{bT}}\int d\mathbf{q}_2 \times \frac{f_{bT}(\mathbf{Q}-\mathbf{q}_2)\,\phi\left(\mathbf{p}_a - \frac{A_a}{A_P}\mathbf{p}_P - \mathbf{q}_2\right)\, f_{aT}(\mathbf{q}_2)}{-\mathbf{q}_2^2 - 2\mathbf{p}_{aX}\cdot\mathbf{q}_2 + i\epsilon} \tag{30}$$

Treating only the singularities of the propagator and using contour integration, we reduce equation (30) to

$$T_D^1 \cong \frac{4\pi i p_{aX}}{V\mu_{bT}}\int_0^\pi \sin\zeta\cos\zeta\, d\zeta\, f_{bT}(\mathbf{Q}-\mathbf{x}) \times \phi\left(\mathbf{p}_a - \frac{A_a}{A_P}\mathbf{p}_P - \mathbf{x}\right)\, f_{aT}(\mathbf{x}) \tag{31}$$

where

$$\mathbf{x} = -2p_{aX}\cos\zeta\,\hat{\mathbf{q}}_2 \tag{32}$$

and $\hat{\mathbf{q}}_2$ is a unit vector.

The singularity structure of the overlap function is ignored here, since only first estimates of the double-scattering corrections are considered. In a

similar manner, we find the double-scattering contribution to the transition matrix of figure 6:

$$T_D^2 \cong \frac{4\pi i p_{bX}}{V \mu_{aT}} \int_0^\pi \sin\zeta \, \cos\zeta \, d\zeta \, f_{aT}(\mathbf{Q} - \mathbf{y}) \times \phi\left(-\mathbf{p}_b + \frac{A_b}{A_P}\mathbf{p}_P + \mathbf{y}\right) f_{bT}(\mathbf{y}) \quad (33)$$

where

$$\mathbf{p}_{bX} = \frac{1}{A_T + A_b}(A_b \mathbf{p}_X - A_T \mathbf{p}_b) \quad (34)$$

and

$$\mathbf{y} = -2 p_{bX} \cos\zeta \, \hat{\mathbf{q}}_2 \quad (35)$$

The approximations to the double-scattering terms given by equations (31) and (33) are evaluated numerically using the inputs described subsequently.

Results and Discussion

We now apply our model to ^{3}He production from 1 GeV/A alpha particles scattering on ^{1}H targets. The treatment of the summation over target states for composite targets is not discussed in this report. General properties of the overlap functions for single nucleon knockout have been reported by Berggren (ref. 16). For the ^{3}He-n overlap, a sum of Yukawa terms is assumed to be

$$\Phi(\mathbf{p}) = \sum_{i=1}^{2} \frac{a_i}{p^2 + \alpha_i^2} \quad (36)$$

with $\alpha_1 = \alpha$, and the normalization is

$$\int |\Phi(\mathbf{p})|^2 d\mathbf{p} = |Z|^2 \quad (37)$$

where $|Z|^2$ is the total probability of finding the two fragments in the projectile. Note from reference 16 that $|Z|^2 < 1$. For ^{3}He-n, $\alpha_1 = 0.846$ fm^{-1} and from reference 15, $\alpha_2 = 1.12$ fm^{-1}, $a_1 = 1$, and $a_2 = -1$. For $|Z|^2$, we use 0.9. Values in the literature for $|Z|^2$ range from 0.6 to 0.9 depending on the method of determination. The dispersion integral is then found to be

$$D(p,q) = \frac{4\pi}{q} \sum_{i,j} a_i a_j \left\{ \tan^{-1}\left(\frac{q/2}{\alpha_i^2 - \alpha_j^2}\right) + \frac{1}{2}\left(\frac{p^2 + \alpha_1^2}{p^2 + \alpha_j^2}\right)\left[\tan^{-1}\left(\frac{\alpha_i q}{\alpha_i^2 + p^2 - \frac{q^2}{4}}\right)\right] + \frac{i}{2}\ln\left[\frac{\alpha_i^2 + (p + q/2)^2}{\alpha_j^2 + (p - q/2)^2}\right]\right\} \quad (38)$$

with

$$D(p,0) = 4\pi \sum_{i,j} a_i a_j \frac{1}{\alpha_i + \alpha_j}\left[1 + \frac{\alpha_1^2 + p^2}{(\alpha_i - ip)(\alpha_j - ip)}\right] \quad (39)$$

We note that solutions of this dispersion integral differ in references 13 through 15.

At high energies we use diffractive approximations to the a-T and b-T scattering amplitudes. For neutron-proton scattering, this is

$$f_{bT}(\mathbf{q}) = \frac{\sigma(\rho + i)k_{NN}}{4\pi} e^{-1/2Bq^2} \quad (40)$$

with the NN scattering parameters listed in table 1. For ^{3}He-proton scattering, we use the Glauber approximation result (ref. 17):

$$f_{aT}(\mathbf{q}) = \sum_{j=1}^{3} \binom{3}{j} (-1)^j \left[\frac{\sigma(1 - i\rho)}{2\pi(R^2 + 2B)}\right]^{j-1} \times \frac{\sigma(1 - i\rho)}{2j} e^{-w_j q^2} \quad (41)$$

where

$$w_j = \frac{6B + (3 - j)R^2}{12j} \quad (42)$$

with the radius $R = 1.51$ fm.

Table 1. NN Parameters at 1 GeV

	σ, mb	B, fm^2	ρ
np	43.7	0.26	-0.26
pp	47.6	.24	-.09

Results for the double-differential cross section at several laboratory angles are shown in figures 9 to 11. The experimental data of reference 18 are shown in figures 10 and 11. The dashed line is the spectator term, equation (22); the dotted line the participant term, equation (23); the dash-dot line the coherent sum of the spectator and participant terms; and the solid line the coherent sum of participant-spectator terms and the double-scattering terms of equations (31) and (33). Single-scattering results include FSI. The double-scattering terms are observed to contribute in a nonnegligible way at 0°. This makes a simple extraction using the distorted-wave-born-approximation of the overlap function from small angle data, as was suggested in reference 19, invalid. The double-scattering approximations of equations (31) and (33) do not neglect the longitudinal

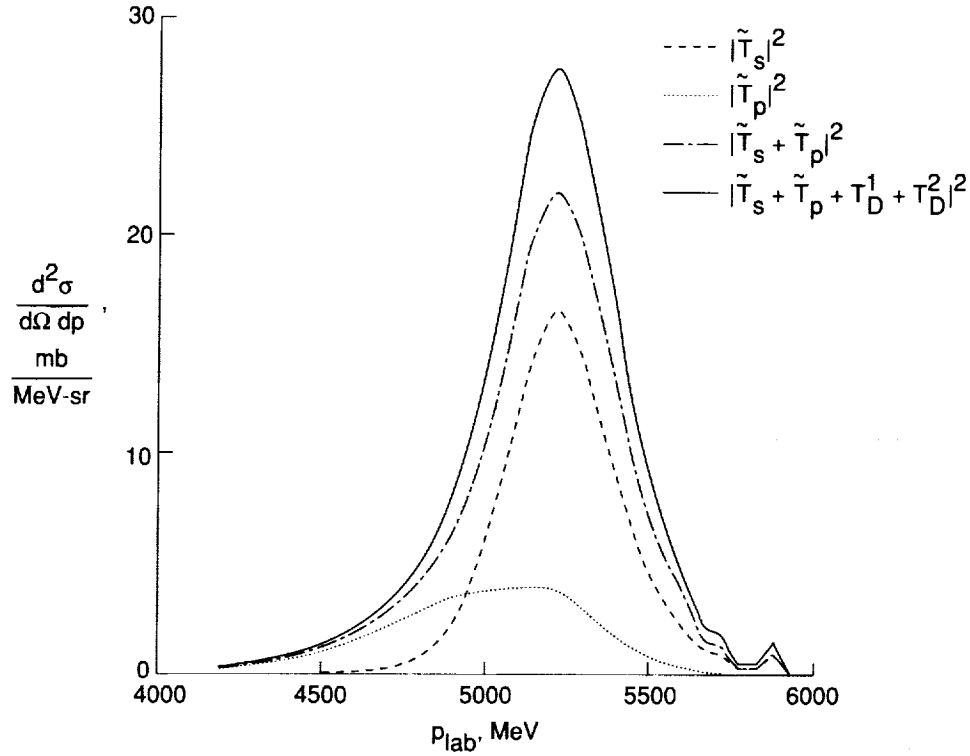

Figure 9. Double-differential cross section at $\theta_{lab} = 0°$ for $\alpha + {}^1H \rightarrow {}^3He$ at 1.02 GeV/A.

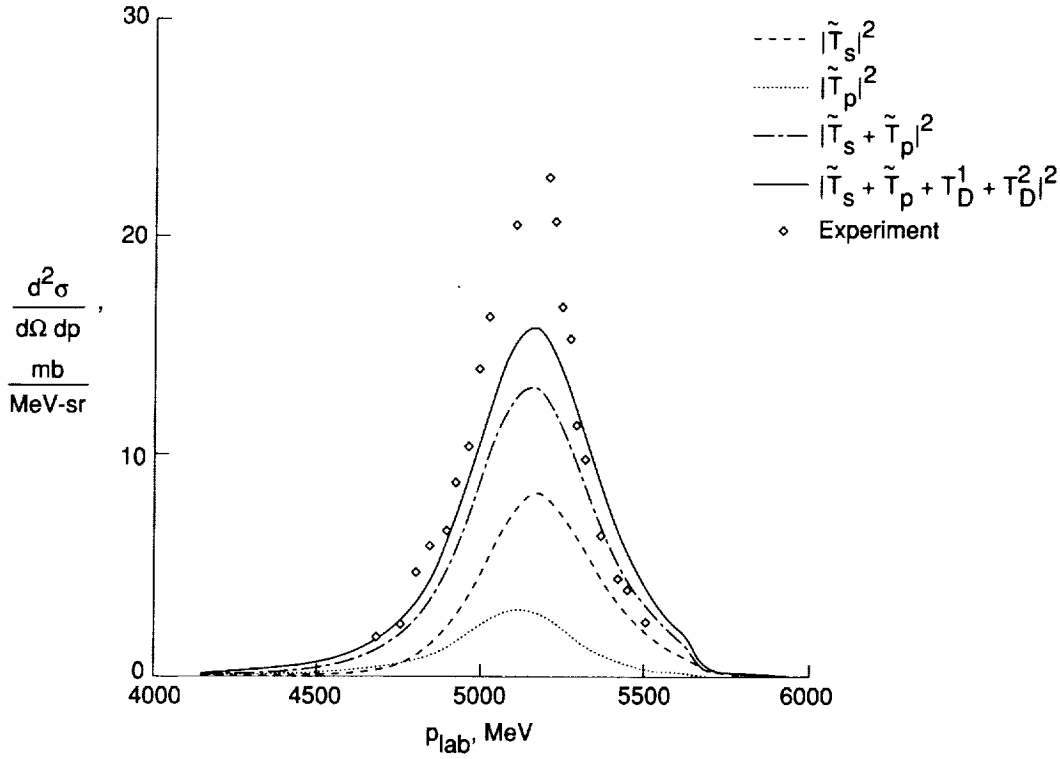

Figure 10. Double-differential cross section at $\theta_{lab} = 0.65°$ for $\alpha + {}^1H \rightarrow {}^3He$ at 1.02 GeV/A. Experimental data from reference 18.

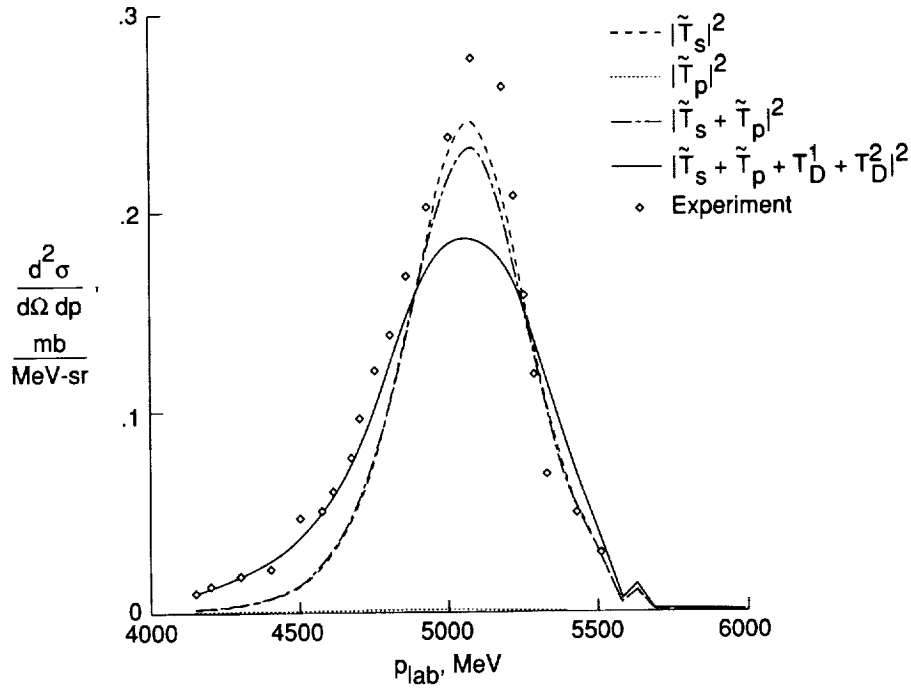

Figure 11. Double-differential cross section at $\theta_{lab} = 4.07°$ for $\alpha + {}^1H \rightarrow {}^3He$ at 1.02 GeV/A. Experimental data from reference 18.

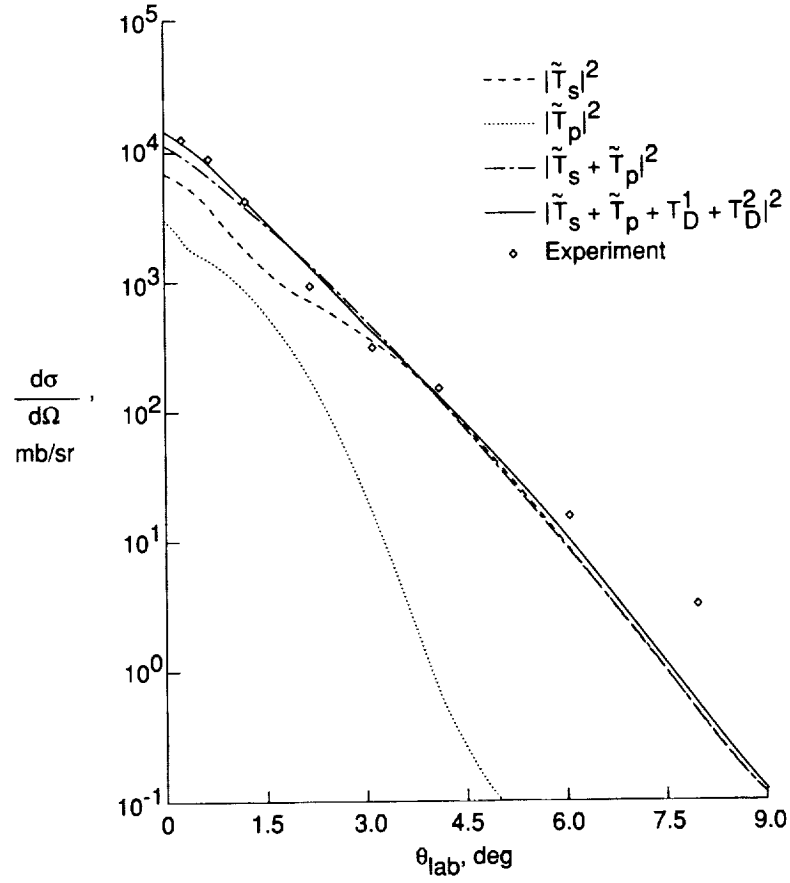

Figure 12. Angular distribution for $\alpha + {}^1H \rightarrow {}^3He$ at 1.02 GeV/A. Experimental data from reference 18.

momentum transfer and therefore lead to a good prediction of the position of the peak in the cross section with increasing angle (as seen in fig. 11 at $\theta_{lab} = 4.07°$). We note that in the Glauber model of alpha-particle breakup of reference 20, the downshift in the momentum distribution must be treated in an ad hoc manner.

Interference effects between the various scattering terms are found in all results. The spectator and participant terms interfere constructively for all angles considered. The energy-dependent parameters ρ_{np} and ρ_{pp} determine the interference effects to a large degree. Prescription for the on-shell fragment-target interaction energy could then be used to study the interference effects in more detail. The singularity structure of the overlap function and FSI effects on the double-scattering terms need to be studied in order to make conclusions about the magnitude and interference contributions of the double-scattering terms.

In figure 12, the angular distribution for ^{3}He production is shown in the laboratory system. The importance of the participant and double-scattering terms is seen at all angles. We expect that the small differences between our calculations and the data at the smallest angles between 1.5° and 4.5° could be reduced if the phases between the various terms were treated correctly. We underestimate the data at the largest angles, which may be because of contributions not treated here, such as intermediate-state deuteron production, charge exchange, and pion production. Results for the total production cross section are given in table 2. Good agreement is found with experiment when all scattering terms are included.

Table 2. ^{3}He Production Cross Section in α + ^{1}H Reaction at 1 GeV/A

	σ, mb
Experiment (ref. 18)	24.1 ± 1.9
$\left\|\widetilde{T}_s\right\|^2$	12.2
$\left\|\widetilde{T}_p\right\|^2$	3.3
$\left\|\widetilde{T}_s + \widetilde{T}_p\right\|^2$	20.7
$\left\|\widetilde{T}_s + \widetilde{T}_p + T_D^1 + T_D^2\right\|^2$	22.7

Conclusions

A first approximation to the double-scattering correction to the participant-spectator model of fragmentation was found to be important in describing alpha-particle breakup. Interference effects between single- and double-scattering graphs were found to determine the overall magnitude and shape of the double- and single-differential production cross sections. The prescription for the on-shell projectile cluster-target amplitude energy should be considered to study the interference effects in more detail. The singularity structure of the projectile dissociation overlap function should be considered to improve the results given here. Good agreement with experiment for the total production cross section was found for the single projectile energy considered. Extensions of this work are expected to contribute to the development of a nuclear cross section data base for galactic cosmic ray transport codes.

NASA Langley Research Center
Hampton, VA 23665-5225
March 12, 1991

References

1. Curtis, Stanley B.: Effects of Low and High LET Radiation on Neoplastic Transformation in Cells and the Importance of Single Track Effects in Space. *Terrestrial Space Radiation and Its Biological Effects,* Percival D. McCormack, Charles E. Swenberg, and Horst Bücker, eds., Plenum Press, 1988, pp. 153–161.

2. Cucinotta, Francis A.; Katz, Robert; Wilson, John W.; Townsend, Lawrence W.; Nealy, John E.; and Shinn, Judy L.: *Cellular Track Model of Biological Damage to Mammalian Cell Cultures From Galactic Cosmic Rays.* NASA TP-3055, 1991.

3. Wilson, J. W.; Townsend, L. W.; and Badavi, F. F.: Galactic HZE Propagation Through the Earth's Atmosphere. *Radiat. Res.,* vol. 109, no. 2, Feb. 1987, pp. 173–183.

4. Townsend, L. W.; and Wilson, J. W.: An Evaluation of Energy-Independent Heavy Ion Transport Coefficient Approximations. *Health Phys.,* vol. 54, no. 4, Apr. 1988, pp. 409–412.

5. Goldhaber, Alfred S.; and Heckman, Harry H.: High Energy Interactions of Nuclei. *Annual Review of Nuclear and Particle Science, Volume 28,* J. D. Jackson, Harry E. Gove, and Roy F. Schwitters, eds., Annual Reviews Inc., 1978, pp. 161–205.

6. Cucinotta, Francis A.: Theory of Alpha-Nucleus Collisions at High Energies. Ph.D. Thesis, Old Dominion Univ., 1988.

7. Cucinotta, F. A.; Townsend, L. W.; and Norbury, J. W.: Corrections to Pole Diagrams in ^{4}He Fragmentation at 1 GeV/A. *Bull. American Phys. Soc.,* vol. 34, no. 4, Apr. 1989, p. 1138.

8. Shapiro, I. S.: Some Problems in the Theory of Nuclear Reactions at High Energies. *Sov. Phys. Uspekhi,* vol. 10, no. 4, Jan.-Feb. 1968, pp. 515–535.

9. Wilson, John W.: Composite Particle Reaction Theory. Ph.D. Diss., College of William and Mary in Virginia, June 1975.

10. Thies, Michael: Quantum Theory of Inelastic Multiple Scattering in Phase Space. *Ann. Phys. (NY),* vol. 123, no. 2, Dec. 1979, pp. 411–441.

11. Norbury, John W.; Townsend, Lawrence W.; and Deutchman, Philip A.: *A T-Matrix Theory of Galactic Heavy-Ion Fragmentation.* NASA TP-2363, 1985.

12. Shapiro, I. S.; Kolybasov, V. M.; and Augst, G. R.: Treiman-Yang Criterion for Direct Nuclear Reactions. *Nucl. Phys.,* vol. 61, no. 3, Jan. 1965, pp. 353–367.

13. Kolybasov, V. M.; and Ksenzov, V. G.: Role of Secondary Rescattering in the Reaction $D(\pi^-, \pi^- p)n$ at High Energies. *Sov. J. Nucl. Phys.,* vol. 22, no. 4, July–Dec. 1975, pp. 372–378.

14. Aladashvili, B. S.; Germond, J. F.; Glagolev, V. V.; Nioradze, M. S.; Siemiarczuk, T.; Stepaniak, J.; Streltsov, V. N.; Wilkin, C.; and Zielinski, P.: Final-State Interaction in the High-Energy Proton-Deuteron Break-Up Reaction. *J. Phys. G.,* vol. 3, no. 1, 1977, pp. 7–20.

15. Chevallier, M.; Fäldt, G.; Hallgren, A.; Jonsson, S.; Badelek, B.; Burq, J. P.; Chemarin, M.; Dahlgren, S.; Grafström, P.; Hagberg, E.; Ille, B.; Kullander, S.; Lambert, M.; Nassalski, J.; Querrou, M.; and Vazeille, F.: Quasi-Elastic Pion-Helium Scattering at 5 GeV/c. *Nucl. Phys.,* vol. A343, no. 3, July 21, 1980, pp. 449–467.

16. Berggren, Tore: Overlap Integrals and Single-Particle Wave Functions in Direct Interaction Theories. *Nucl. Phys.,* vol. 72, no. 2, Oct. 1965, pp. 337–351.

17. Glauber, R. J.; and Matthiae, G.: High-Energy Scattering of Protons by Nuclei. *Nucl. Phys.,* vol. B21, no. 1, Aug. 1, 1970, pp. 135–157.

18. Bizard, G.; Le Brun, C.; Berger, J.; Duflo, J.; Goldzahl, L.; Plouin, F.; Oostens, J.; Van Den Bossche, M.; Vu Hai, L.; Fabbri, F. L.; Picozza, P.; and Satta, L.: ^{3}He Production in ^{4}He Fragmentation on Protons at 6.85 GeV/c. *Nucl. Phys.,* vol. A285, no. 3, Aug. 1, 1977, pp. 461–468.

19. Fujita, T.; and Hüfner, J.: Momentum Distributons After Fragmentation in Nucleus-Nucleus Collisions at High Energy. *Nucl. Phys.,* vol. A343, no. 3, July 21, 1980, pp. 493–510.

20. Bizard, G.; and Tekou, A.: Interpretation of the ^{4}He Dissociation at High Energy. *Nuovo Cimento,* vol. 51A, no. 1, May 1, 1979, pp. 114–130.

NASA
National Aeronautics and Space Administration

Report Documentation Page

1. Report No.	2. Government Accession No.	3. Recipient's Catalog No.
NASA TM-4262		

4. Title and Subtitle	5. Report Date
Corrections to the Participant-Spectator Model of High-Energy Alpha-Particle Fragmentation	May 1991
	6. Performing Organization Code
7. Author(s)	8. Performing Organization Report No.
Francis A. Cucinotta, Lawrence W. Townsend, John W. Wilson, and John W. Norbury	L-16883
9. Performing Organization Name and Address	10. Work Unit No.
NASA Langley Research Center Hampton, VA 23665-5225	199-04-16-11
	11. Contract or Grant No.
12. Sponsoring Agency Name and Address	13. Type of Report and Period Covered
National Aeronautics and Space Administration Washington, DC 20546-0001	Technical Memorandum
	14. Sponsoring Agency Code

15. Supplementary Notes

Francis A. Cucinotta, Lawrence W. Townsend, and John W. Wilson: Langley Research Center, Hampton, Virginia.
John W. Norbury: Rider College, Lawrenceville, New Jersey.

16. Abstract

The participant-spectator model of nuclear fragmentation is described in terms of pole graphs from direct reaction theory. Corrections to the model for more than one projectile fragment scattering on the target are considered using a triangle graph model. Results for alpha-particle fragmentation at 1 GeV/A indicate that corrections to the participant-spectator model are significant, as indicated by the large interference effects found between the pole and triangle graph terms in the double- and single-differential cross sections.

17. Key Words (Suggested by Author(s))	18. Distribution Statement
Nuclear fragmentation Inclusive momentum distribution Participant-spectator models	Unclassified—Unlimited Subject Category 73

19. Security Classif. (of this report)	20. Security Classif. (of this page)	21. No. of Pages	22. Price
Unclassified	Unclassified	12	A03

NASA FORM 1626 OCT 86

NASA-Langley, 1991

For sale by the National Technical Information Service, Springfield, Virginia 22161-2171